01,07

Influence of external influences on the creep of aluminum alloys with microscopic inclusions at room temperatures

© P. Friha[1], D.E. Pshonkin[1], P.A. Skvortsov[2], V.K. Nikolaev[1], A.A. Skvortsov[1,¶]

[1] Moscow Polytechnic University,
Moscow, Russia
[2] Blagonravov Institute of Machine Science, Russian Academy of Sciences,
Moscow, Russia

¶ E-mail: skvortsovaa2009@yandex.ru

Received December 6, 2022
Revised December 6, 2022
Accepted February 21, 2023

It is devoted to the experimental study of the creep of an aluminum alloy containing microscopic inclusions. It was found that preliminary electric ignition ($j < 3 \cdot 10^6$ A/m^2) of the material leads to an increase in the creep of the samples. The reasons for the observed changes are associated by the authors with the formation of local areas of high mechanical stresses near the interface of the inclusion — matrix interface. The assessment of the level of emerging local thermoelastic stresses in aluminum $\delta_T \sim 35$ MPa, as well as the characteristic size of such areas ($\sim 2\,\mu$m). The observed increase in creep is determined by the resultant effect of residual stresses and stresses of thermal nature, which contributes to the creation of additional local sources of deformation in the interfacial regions. Local stress concentrators lead to a local increase in the number of mobile dislocations, which is the main reason for the change in the mechanical properties of the aluminum alloy under consideration with microscopic inclusions.

Keywords: Aluminum alloys, plastic deformation, creep, phase interface, dislocation dynamics.

DOI: 10.21883/PSS.2023.04.55988.549

1. Introduction

Current tasks in the field of material physics require continuous improvement of material processing methods to improve their performance. This demand exists for the continuous improvement of efficiency of modern production, which is determined by the improvement of quality of products made of metals and alloys, the development and application of new technological methods of material processing. It is well known, that many technological methods result in plastic deformation of samples under applied external mechanical stresses. This results in changes in internal structure of materials connected with the dynamics of grains, particles of the second phase, pores, migration of linear and pinpoint structural defects.

In addition to mechanical impacts, the defects of internal structure of metals and alloys can be significantly affected by thermal electric and magnetic fields (electroplastic [1,2], magnetoplastic effects [3,4], laser methods of material processing [5] etc.), which can be used to develop new methods to control structure-sensitive properties of metals and alloys.

Foe example, one of promising methods of aluminum alloy processing is laser building-up [5]. The extreme thermal conditions (created by laser heating) in the heat treatment zone promote formation of alloys with complex compositions. Microstructure of these regions has been investigated by scanning and transmission electron microscopy. The investigation has shown the presence of inclusions in them based on $MgZn_2$ and CuMgZnAl. In addition, cavities can be formed at the interface of the regions in question as well. Thus, the impacts of this type result in formation of bulk inclusions in the alloys.

Also, a considerable number of studies have been focused on the formation and dynamics of inclusions in aluminum and its alloys. For example, in [6] mechanisms of single-crystal aluminum deformation have been studied under uniaxial stretching in the presence of inclusions based on magnesium and titanium. The authors have observed a change in mechanical properties of Al in the presence of inclusions (spherical particles have been added in the form of Al crystals in the process of material production). When adding Mg-based inclusions, a high level of mechanical stress has been observed at the Al−Mg interface and absence of the dislocation mobility. This has been resulted in quick destruction of the crystal in the presence of such inclusions. As for Al crystals with Ti-based inclusions, a lower level of mechanical stress has been observed at the Al−Ti interphase boundary. In addition, in the presence of Ti-inclusions a high mobility of dislocations has been observed that promoted the predominance of plastic material destruction mechanisms [6]. Also, the mechanisms of destruction of plastic materials with inclusions have been discussed in [7]. The authors have determined experimentally the local conditions to form cavities for individual inclusions located in front of a crack. In addition, the conditions of cavity formation in the matrix

have been investigated in the presence of different sizes of inclusions [7].

As for materials with ferromagnetic inclusions, they are close in terms of their properties to so-called magneto-rheologic materials. In the later the key role is played by „magnetoactive" particles added to the matrix. The presence of such particles in the material allows reversibly changing its physico-mechanical properties under the effect of external magnetic field [4]. Returning to aluminum materials, it is worth emphasizing that iron-containing zones can be formed at the stage of secondary aluminum processing [8]. It is known that the secondary aluminum contains many impurity elements, such as Fe, Si, Mg, etc. Due to the low solubility of Fe atoms in the solid aluminum, these atoms tend to bind with aluminum during crystallization in the form of inclusions that are intermetallic compounds rich in Fe. Such inclusions have a significant effect on mechanical and casting properties of aluminum alloys [8]. The effects of different shape of inclusions on the creep and fatigue processes in materials have been investigated in [9]. The authors have shown that, for example, elliptic inclusion results in a higher stress concentration at the interphase boundary (as compared to spherical inclusion).

In addition to magnetic fields, the structure and properties of aluminum alloys are noticeably affected by electric impact [10,11]. For example, a pulse impact of induced current on the mechanical properties and microstructure of the Al−Zn−Mg−Cu alloy has been closely studied by transmission electron microscopy, x-ray diffraction and measurements of electron backscatter diffraction [11]. The experimental results have shown that after the induced electric pulse treatment the strength and the density of dislocations of the alloy decreases and the relative elongation increases significantly. In addition, an insignificant increase in grain size and size of the second phase particles takes place. The authors have made a conclusion that the observed changes in mechanical properties and microstructure of the material are related to the Joule effect and purely electric effects that increase the concentration of vacancies and the coefficient of diffusion of atoms of the dissolved substance promoting the recovery of dislocations, the growth of deposition phase and the rotation of grains [11].

In addition to the direct application of the electric pulse technique to metals and alloys, the use of pulse magnetic fields has been studied to control the microstructure and mechanical properties of aluminum alloys [12,13]. The physics of magnetic field effect is related by the authors to induced electric currents, the Lorentz force and the Joule heating effects. However, the study contains no detailed investigation of the interaction mechanics.

Thus, the effect of electric and magnetic fields on aluminum alloys with complex chemical composition is of interest in terms of both the identification of interaction micromechanics in a multiphase medium and the possibility to develop new methods to control its structure-sensitive properties. Therefore, this study will be focused on the effect of direct current on the features of creep processes in aluminum alloys with iron-based microscopic ferromagnetic inclusions.

2. Materials and research methods

Specimens of polycrystalline aluminum cut off a flat tape in the form of hourglass with the working part size of $80 \times 5 \times 2$ mm were used as subjects of the research. The alloy under study was creep-tested using a WP-600 lever-type creep testing machine. In the process of measurements (at room temperature), concurrently with the application of load (in a stepwise manner) elongation of the specimen was measured by micrometer (with a measuring sensitivity of $10\,\mu$m), at each step of loading. The test setup provided constancy of the load in the process of measurement and smoothness of the loading-unloading. The specimens were isothermally annealed in the air on a heating table with a maximum temperature of up to $T = 473$ K. The microstructure of specimens was investigated using optical, scanning and transmission electron microscope. The direct current ($j_{\max} = 2 \cdot 10^6$ A/m^2, $t_{\max} = 60$ minutes) was applied using a standard power supply unit. Then the current-treated specimens and check-specimens were creep-tested. The maximum temperature of specimens of this annealing was not more than 373 K.

The presence of iron-containing inclusions was confirmed by optical and transmission electron microscopy (a foil was used with a thickness of $100\,\mu$m). A typical TEM-image is shown in Fig. 1, where Fe-inclusions are outlined with light areas. The obtained atomic spectra are indicative of the presence of iron inclusions (~ 34 at.%) and aluminum (~ 47 at.%). In addition, impurities of B (~ 8 at.%), Si (~ 6 at.%), Mn (~ 1 at.%) and O (~ 3 at.%) have been found in the inclusion. The average grain size in specimens was $\sim 60\,\mu$m and the average inclusion size was $x_i = 5\,\mu$m.

Magnetic properties of specimens with iron-containing inclusions were confirmed through the investigations by a SQUID-magnetometer that helped to detect a magnetic hysteresis with a coercive force of 278 kA/m [15].

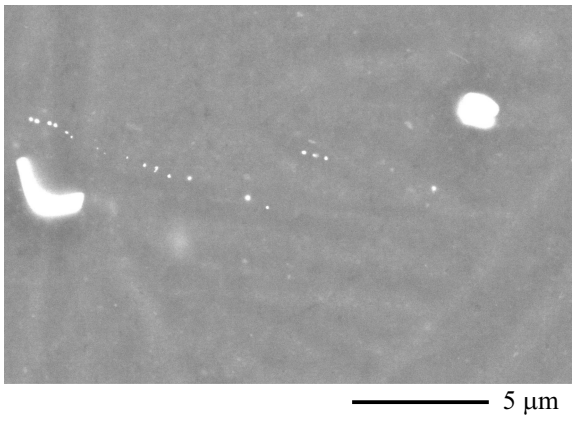

Figure 1. TEM-photo of microstructure of the specimen with inclusions under study.

3. Analysis of obtained results

Previously [14,15] an effect of static magnetic fields on mechanical properties of the material with inclusion in question has been found. Thus, after an exposure of specimens to a static magnetic field with an induction of 0.7 T the creep rate of polycrystalline Al with inclusions of Fe_xAl_{x-1} increases by up to 25%. This has been also confirmed on the specimens used in this study.

One of the most probable explanations for the observed magnetoplasticity consists in the high magnetostriction constant of the Fe_xAl_{1-x} alloy taken into consideration. Estimates of mechanical stresses arising near the ferromagnetic inclusions under the effect of their magnetostriction (~ 650 MPa) show that these stresses are sufficient to form zones of newly introduced dislocations around the inclusion when the specimen is paced in a magnetic field [15].

Thus, the processes near interphase boundaries are the cause of the change in mechanical properties of the aluminum matrix. Therefore, other external impacts that can have an effect on the state of inclusion–matrix interphase boundaries will result in a change in mechanical properties of the crystal. One of such impact is electric current. It is well known that it is the directed motion of charged particles that is a key factor of formation and migration of molten inclusions [16], including those in aluminum polycrystals [17]. Therefore, in the following text the effect of electric current on the process of plastic deformation during creep tests of specimens will be considered.

Results of the material creep studying have shown that after the electric current has flown through the Al-alloy,

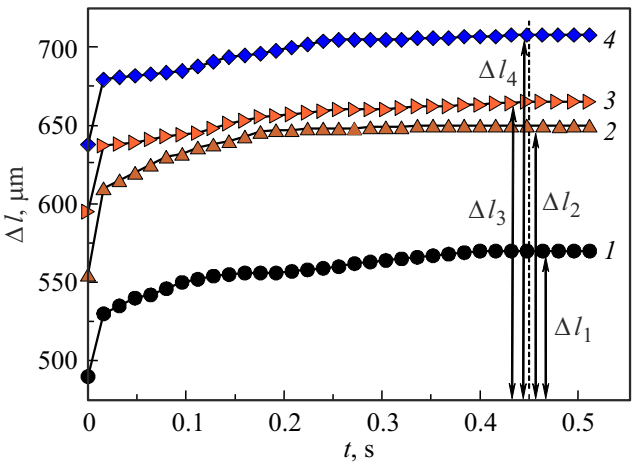

Figure 2. Creep deformation curves of specimens under uniaxial stretching with an external load of $\sigma = 150$ MPa at room temperature. Before deformation: *1* — check-specimen without additional external impacts; *2* — specimen after treatment by an electric current of $j = 2 \cdot 10^6$ A/m^2 for 30 min in the air, specimen temperature in the process of treatment was 333 K; *3* — specimen after annealing at $T = 333$ K for 30 min in the air; *4* — specimen after preliminary exposure to a static magnetic field at room temperature for 30 min in the air at room temperature.

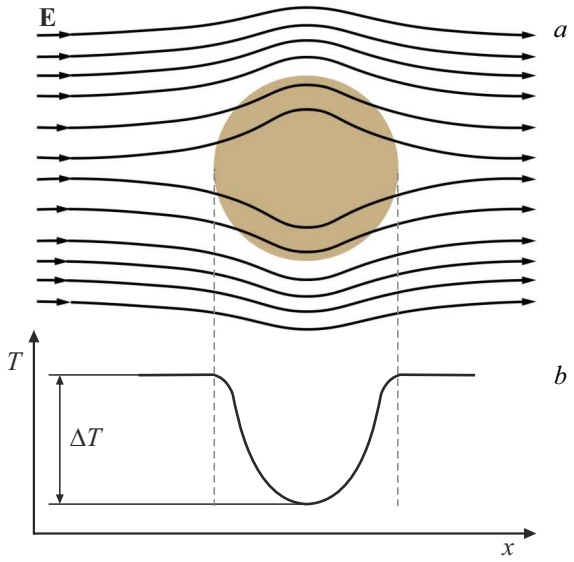

Figure 3. Image of electric field strength lines in a medium with inclusion (a) and temperature distribution in the inclusion and at the inclusion–matrix interface (b).

the specimens have demonstrated an increase in the creep property by 15% (Δl_2, Fig. 2) as compared to the check-specimens (Δl_1, Fig. 2). At the same time, it should be noted that specimens have demonstrated a higher creep property a simple annealing (at the same temperature of $T = 333$ K as with the electric current) (Δl_3, Fig. 2).

To estimate the stresses arising at the inclusion-to-aluminum matrix interfaces under current flowing, thermal gradients were considered that arise due to the difference between specific resistances of the matrix ρ_m and the inclusion ρ_i. The difference between ρ_m and ρ_i of the inclusion results in the appearance of local regions with non-uniform heat emission (Fig. 3). The heat emitted in a conductor with current flow is determined by the following formula:

$$w = \sigma E^2, \tag{1}$$

where $\sigma = \frac{1}{\rho}$ is conductivity of the medium, ρ is specific resistance; E is electric field strength. The value of E_i in the inclusion was calculated by the following relationship [18]:

$$E_i = \frac{3\rho_i}{2\rho_i + \rho_m} E_m, \tag{2}$$

where E_m is electric field strength in the matrix with flow of electric current with a density of $j = 2 \cdot 10^6$ A/m^2.

Calculations of the field strength give the following values: $E_m = 5.6 \cdot 10^{-3}$ V/m for the matrix and $E_i = 7.3 \cdot 10^{-3}$ V/m for inclusions at specific resistances of $\rho_m = 2.7 \cdot 10^{-8}\ \Omega \cdot$ m for the matrix and $\rho_i = 9.7 \cdot 10^{-8}\ \Omega \cdot$ m for inclusions.

The performed estimates show that in the initial moments of current flowing the matrix is warmed stronger than the inclusion, which may be the cause of the temperature gradient at the matrix–inclusion interphase boundary. However,

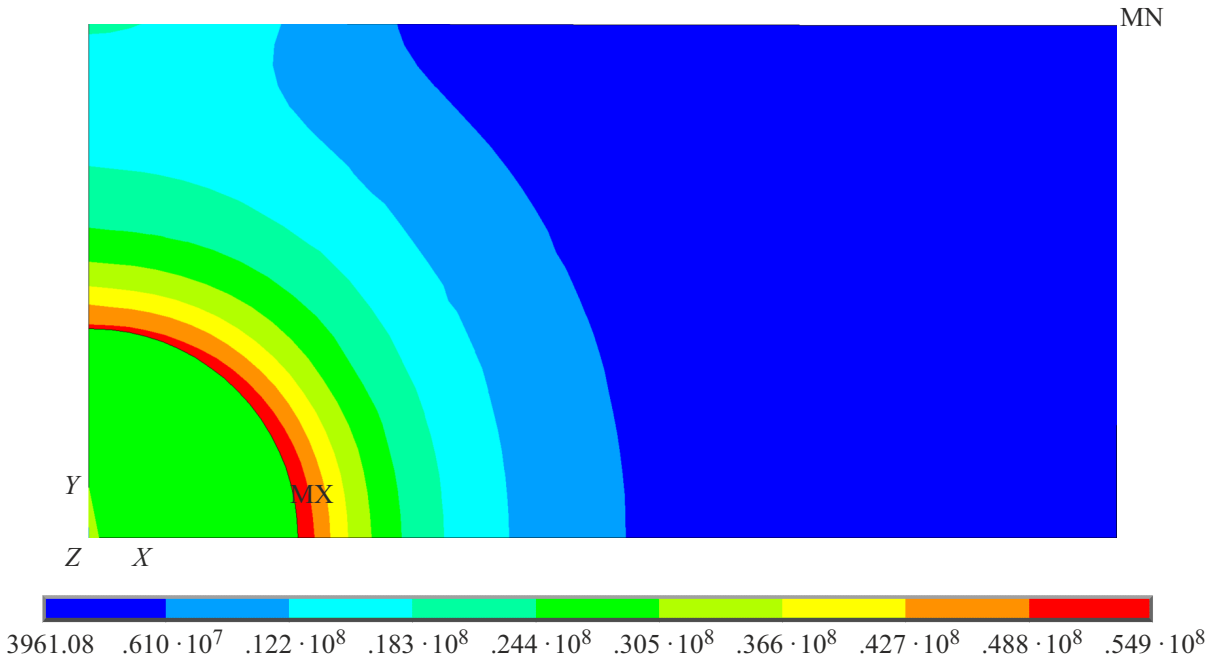

Figure 4. Results of the numerical modeling of thermal stresses in the two-phase metal system at a steady temperature of $T = 333$ K.

based on the estimate of typical heating time of inclusion with an average size of x_i during the exposure time τ_i according to the following equation:

$$x_i = \sqrt{a_i \tau_i}, \tag{3}$$

(where $a = 30 \cdot 10^{-6}$ m^2/s is temperature conductivity of the inclusion [19]), it has been shown that the typical time τ_i is of order of magnitude of microseconds. Therefore, the thermal inhomogeneities at the turn-on moment give no significant contribution to the mechanical properties of the matrix.

To estimate the mechanical stresses in aluminum near the inclusions, the known estimate is used [20]:

$$\sigma_m = E_m(\alpha_m - \alpha_i)\Delta T. \tag{4}$$

Hereinafter $E_m = 71$ GPa, $\alpha_m = 24 \cdot 10^{-6}$ 1/K, $\alpha_i = 12 \cdot 10^{-6}$ 1/K are modulus of elasticity, coefficients of linear thermal expansion of the aluminum alloy and the material, respectively [19]. The estimate by equation (4) for the matrix–inclusion system under consideration gives values of the arising thermal stresses in the matrix of $\sigma_m = 35$ MPa ($\sigma_{0.2} = 60$ MPa for the Al-alloy [19]). This relationship does not take into consideration thicknesses of material and non-linear behavior of the dependence of α_m and α_i on temperature.

To additionally estimate the thermoelastic stresses arising in the aluminum matrix in the presence of inclusions, numerical modelling was applied using finite element analysis in the Ansys software. The problem statement and model build-up assumed that the specimen with inclusions in the process of external impact is heated uniformly up to a temperature of $T_2 = 333$ K (the initial temperature of the system was taken equal to $T_1 = 293$ K). The temperature load in the model was set in this way. The plate was secured along its perimeter. Parameters of materials of the matrix and the inclusion used as an input for the calculation model are summarized in the table.

Parameters of materials used for the mathematical modeling

Material	K, W/(m · K)	C, J/(kg · K)	α, 1/R
Al	237	897	$24 \cdot 10^{-6}$
Fe	80.4	460	$12 \cdot 10^{-6}$

The temperature problem was solved using the plane 55 element (the element has four nodes with a single degree of freedom at each node; as a rule, it is applied in the modeling of 2-D, steady-state or transient thermal analysis). The strength problem was solved with the use of the plane 182 element (the element is used to model 2-D solid structures when modeling deformations of elastic materials; as a rule, it is defined by four nodes with two degrees of freedom at each node: translations in the nodal x and y directions). The calculation used 2462 elements and 2534 nodes. The modeling results are shown in Fig. 4.

It can be easily seen that the stresses arising in the calculation model under study at the given temperature mode are consistent with the estimates made in accordance with equation (3). Graphs of the stress distribution in the region of inclusion–matrix interphase boundary are shown in Fig. 5. The obtained results of the calculation make it possible to determine typical size of the zone

(near the interphase boundary) with the maximum level of mechanical stresses and deformations of $x_d \sim 2\,\mu$m.

Thus, in the specimens under consideration the arising thermoelastic mechanical stresses $\sigma_T \approx \sigma_m$ are lower than the $\sigma_{0.2}$ stresses of the plastic deformation start.

However, the experimentally observed dependencies are indicative of the increase in creep property of specimens after both the simple isothermal annealing and the electroannealing. To explain the observed experimental results, it is necessary to take into account that the resulting mechanical stress acting in the crystal σ_{in}

$$\sigma_{in} = \sigma_s + \sigma_T \tag{4}$$

is composed of residual stresses in the material σ_s (due to the production process of the strip by the hot-rolling method) and stresses of thermal nature σ_T. Therefore, the resulting σ_{in} may be considerably higher than the stress $\sigma_{0.2}$ of the matrix.

In this case dislocations will be generated in the matrix, which gliding will result in a plastic deformation at the following rate (as compared with the non-annealed specimen) [21]:

$$\dot{\varepsilon} = \rho_d b v_d, \tag{5}$$

and, as a consequence, in an increase in the creep property. Here ρ_d is density of dislocations, b is modulus of the Burgers vector, v_d is dislocation rate.

The relaxation of residual stresses in this case is determined by the temperature of annealing and not by its duration [21]. With stresses σ_{in} less than yield strength no massive multiplication of dislocations and massive gliding of dislocations takes place. Slow plastic flowing is implemented through movement of a limited number of easy movable dislocations in the action field of various obstacles (pinpoint defects, dislocation tangles, disperse particles, grain boundaries).

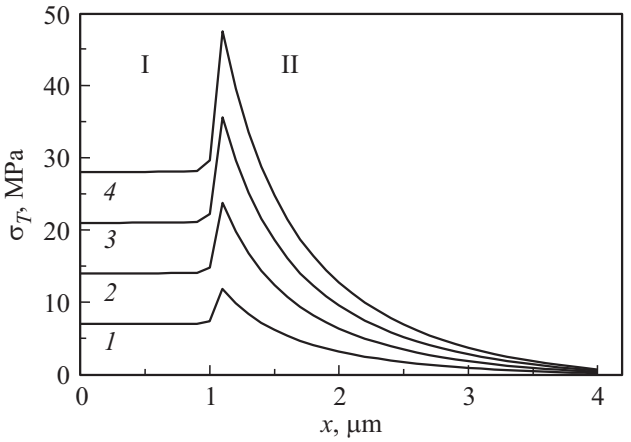

Figure 5. Stress distribution along the length of specimen (I — inclusion zone, II — matrix) at steady temperatures: *1* — $T_1 = 303$ K; *2* — $T_2 = 313$ K; *3* — $T_3 = 323$ K; *4* — $T_4 = 303$ K. The coordinate origin corresponds to the geometric center of the inclusion.

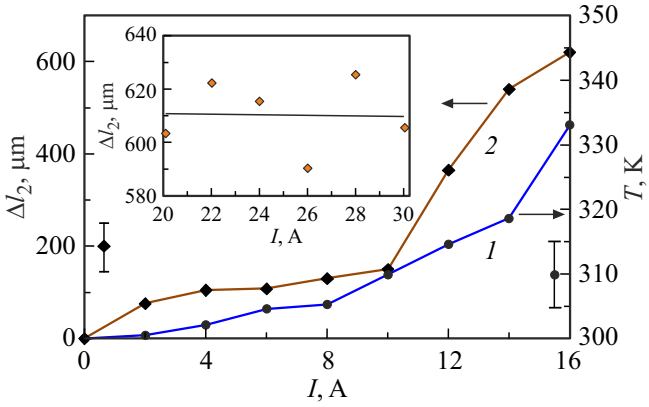

Figure 6. Dependence of specimen temperature (*1*) and absolute elongation (*2*) on the electric current amperage. The cross-section of specimens was 5×2 mm. In the insert: dependence of the absolute elongation of specimen on the amperage of current through it at a constant temperature of $T = 333$ K.

It is worth emphasizing that experiments has not identified any significant differences between the effect of preliminary isothermal annealing ($T < 335$ K) of specimens and their electroannealing ($j < 3 \cdot 10^6$ A/m^2), which is indicative of the „thermal" nature of the electric current impact. To confirm this, a number of experiments were conducted where specimen temperature was fixed but the electric current density varied. Results of this series of experiments are shown in the insert to Fig. 6. It can be seen, that at a fixed specimen temperature of $T = 333 \pm 5$ K a change in the current density j through the specimen does not result in a noticeable change in the behavior of the material creep property (insert, Fig. 6).

In the case of electroannealing without heat removal the increase in j promoted heating of the specimen and with further loading it resulted in an increase in its creep property (Fig. 6).

4. Conclusion

The study has considered issues of creep properties of an aluminum alloy with iron-containing inclusions. It has been shown experimentally that preliminary impact (exposure to a static magnetic field, flowing of direct current, isothermal annealing) before the creep test of specimens promotes increase in the creep property. The observed changes are related to the regions of local plastic deformation near the inclusion–matrix interphase boundary. Based on results of calculations and mathematical modeling the arising thermoelastic stresses of $\sigma_T \sim 35$ MPa were estimated by the method of finite-element analysis. The study notes that the observed increase in the creep property is determined by the resulting action of residual stresses and stresses of the thermal nature. The obtained estimates show that the preliminary electroannealing of specimens promotes creation of additional local sources of deformation at interphase regions

that result in a local increase in the number of movable dislocations. Based on the numerical modeling an estimate of character and size of these regions ($\sim 2\mu$m) has been made. It has been noted that thermoelastic deformations at the interphase boundary may be the main cause of the change in mechanical properties of multiphase metal materials with microscopic inclusions.

Funding

The work was carried out within the framework of the state assignment of the Ministry of Education and Science to universities (application reg. No. 1022040800179-4).

Conflict of interest

The authors declare that they have no conflict of interest.

References

[1] Y.-C. Liu, S.-K. Lin. JOM **71**, *9*, 3094 (2019).
[2] X. Zhang, S. Xiang, K. Yi, J. Guo. Acta Metallurgica Sinica **58**, *5*, 581 (2022).
[3] A. Kumar, A. Arockiarajan. J. Magn. Magn. Mater. **546**, 168821 (2022).
[4] M.H. Ahmad Khairi, S.A. Mazlan, N.M. Hapipi, N. Nordin. Adv. Eng. Mater. **21**, *3*, 1800696 (2019).
[5] J. Wang, I. Timokhina, K. Sharp, A. Shekhter, Q. Liu. Surf. Coatings Technol. **445**, 128726 (2022).
[4] S.-H. Peng, J.-J. Yang, Y. Li. J. Plasticity Eng. **21**, *3*, 85 (2014).
[5] A. Lebied, B. Necib, M. Sahli. Mech. Mech. Eng. **21**, *2*, 233 (2017).
[6] A. Rajput, P.S. Kumar. J. Alloys Comp. **869**, 159213 (2021).
[7] I. Sabirov, O. Kolednik. Scripta Mater. **53**, *12*, 1373 (2005).
[8] Y. Sun, X. Huang, C. Liu, M. Zhou, Z. Xinfang. J. Alloys Comp. **934**, *10*, 167903 (2023).
[9] N. Hou, K. Yang. Proced. Eng. **17**, 292 (2011).
[10] O.B. Skvortsov, V.I. Stashenko, O.A. Troitsky. Lett. Mater. **11**, *4*, 473 (2021).
[11] A. Xiao, C. Huang, X. Cui, Z. Yan, Z. Yu. J. Alloys Comp. **911**, 165021 (2022).
[12] J. Luo, H. Luo, C. Liu, T. Zhao, R. Wang, Y. Ma. Mater. Sci. Eng. A **798**, 139990 (2020).
[13] D. Du, James C. Haley, A. Dong, Y. Fautrelle, D. Shu, G. Zhu, X. Li, B. Sun, E. Lavernia. J. Mater. Des. **181**, 107923 (2019).
[14] A. Skvortsov, D. Pshonkin, E. Kunitsyna, R. Morgunov, E. Beaugnon. J. Appl. Phys. **125**, *2*, 023903 (2019).
[15] A.A. Skvortsov, D.E. Pshonkin, M.N. Luk′yanov, M.R. Rybakova. J. Mater. Res. Technol. **8**, *3*, 2481 (2019).
[16] A.A. Skvortsov, N.A. Khripach, B.A. Papkin, D.E. Pshonkin. Microelectron. Int. **35**, *4*, 197 (2018).
[17] A.A. Skvortsov, V.E. Muradov, E.A. Kashtanova. Tech. Phys. Lett. **37**, *6*, 507 (2011).
[18] D.K. Belaschenko, A.M. Orlov, V.I. Parkhomenko, Neorgan. materialy **11**, *10*, 1728 (1975). (in Russian).
[19] Fizicheskiye velichiny. Spravochnik / eds I.S. Grigoriyev, Ye.Z. Meylikhov, Energoatomizdat, M., (1991), 1232 p. (in Russian).
[20] L.S. Sinyov, Nauka i obrazovanie, MGTU im. N.E. Baumana, M. **12**, 946 (2014). (in Russian).
[21] A.N. Orlov, Vvedeniye v teoriyu defeltov v kristallakh, Vyssh. shk., M., (1983), 144 p. (in Russian).

Translated by Y.Alekseev